Supplementary Information

A smart probe for simultaneous imaging of lipid/water microenvironment in atherosclerosis and fatty liver

Zixuan Zhan†[a], Weihua Zhuang†[b], Qian Lei[a], Shufen Li[b], Wuyu Mao[a]*, Mao Chen[b]* and Weimin Li[a]*

[a] Department of Respiratory and Critical Care Medicine, Targeted Tracer Research and Development Laboratory, Precision Medicine Key Laboratory of Sichuan Province & Precision Medicine Center, West China Hospital, Sichuan University, Chengdu, Sichuan, 610041, China.

[b] Laboratory of Heart Valve Disease, Department of Cardiology, West China Hospital, Sichuan University, Chengdu, Sichuan, 610041, China.

† These authors contributed equally to this work

Content

1.General Experimental Section

Materials and Instrumentations

Unless otherwise noted, materials were obtained from commercial suppliers and were used without further purification. ^{1}H NMR, ^{13}C NMR spectra were measured on a Bruker AM400 NMR spectrometer. Proton Chemical shifts of NMR spectra were given in ppm relative to internals reference TMS (^{1}H, 0.00 ppm). HRMS spectral data were recorded on a Bruke Daltonics Bio TOF mass spectrometer. Absorption spectra and photoluminescence spectra were performed on a U-2910 and a Hitachi F-7000 fluorescence spectrophotometer, respectively. Cell and tissue imaging were performed with a Nikon Ni-E multiphoton laser scanning confocal microscope (CLSM).

Cell Cytotoxicity Assay

The cytotoxicity was evaluated by MTT assay. L929 cells and RAW 264.7 cells were cultured in dulbecco's modified Eagle's medium (DMEM) containing 10% fetal bovine serum in 96-well microplates at 37°C under 5% CO_2 atmosphere for 24 h. Then, the culture mediums were replaced with fresh medium containing various concentrations of **LDs-DM** (1, 5, 10, 15 and 20 μM), cells were cultured for another 24 h. Afterwards, MTT reagent was added with final concentration of 0.5 mg/mL, cells were incubated for 4 h at 37°C. Afterwards, the culture mediums were removed and 150 μL DMSO was added to each well to dissolve the formazan. Finally, the absorbance at 490 nm was measured by multi-detection microplate reader.

Cells imaging experiments.

To study the lipid droplets (LDs) specific imaging ability of **LDs-DM**, RAW 264.7 cells were first incubated in glass bottom dishes for 24 h. Then, the culture medium was removed and replaced with serum-free culture medium containing 10 μM oleic acid. After incubating for 2 h, RAW 264.7 cells were washed with PBS for three times and treated with new culture medium containing 1 μM **LDs-DM** for another 1 h. Afterward, the cells were further stained with Nile red (1 μM, in serum-free culture medium) for 0.5 h after the culture medium was

removed. Finally, the cells were washed with PBS for another three times and imaged by CLSM.

To further investigate the LDs imaging ability of **LDs-DM**, RAW 264.7 cells incubated in culture dishes were treated with 10 μM oleic acid for 2 h, and then stained with different concentrations of **LDs-DM** (500 nM, 100 nM and 20 nM) for 1 h and Nile red for 0.5 h, respectively. Finally, the cells were washed with PBS for three times and imaged by CLSM.

To explore the imaging ability of **LDs-DM** in revealing aqueous/lipid interfaces or observing cell microstructure, **LDs-DM** was used for LDs staining (500 nM) in RAW 264.7 cells with oleic acid treated. The fluorescence signals of **LDs-DM** were collected in FITC channel (λ_{em} = 500-550 nm) and Cy5 channel (λ_{em} = 663-738 nm), respectively.

General procedure for animal disease tissues imaging.

All animal experiments were approved by the Sichuan Provincial Committee for Experimental Animal Management (2020339A) and performed according to the institutional and NIH guidelines for the care and use of research animals. Both Balb/c femal mice and genetically engineered apo-lipoprotein E-deficien ApoE-/- (male) mice were fed on a high-fat diet. The disease tissues were stained with **LDs-DM** (500 nM) and Nile red (1 μM) for 1 h or stained with **LDs-DM** (500 nM) only.

Fatty liver and atherosclerotic mice model.

Balb/c femal mice were subcutaneously injected with 200 μL olive oil containing 0.3% tetrachloromethane (mass ratio) every seven days (three times in total). After three weeks, mice were sacrificed, the livers were isolated and washed with PBS immediately, followed by staining with **LDs-DM** and Nile red or only **LDs-DM**. Moreover, some of the hepatic tissues were fixed with paraformaldehyde solution to further perform hematoxylin and eosin (H&E) staining and oil red staining.

ApoE-/- (female) mice were housed in SPF class animal facility and fed on a high-fat diet for 12 weeks. Mice were sacrificed, the entire arterial tree was harvested and longitudinally opened, followed by staining with **LDs-DM** and Nile red or only **LDs-DM**.

Differentiate the normal human liver tissues from patient tissues with fatty liver.

The samples were supported by West China Biobanks, Department of Clinical Research, West China Hospital of Sichuan University. The obtained tissues were stained with **LDs-DM** (500 nM) in PBS for 1 h. After being rinsed three times with PBS, the tissues were imaged with CLSM.

2.Synthesis of Compounds

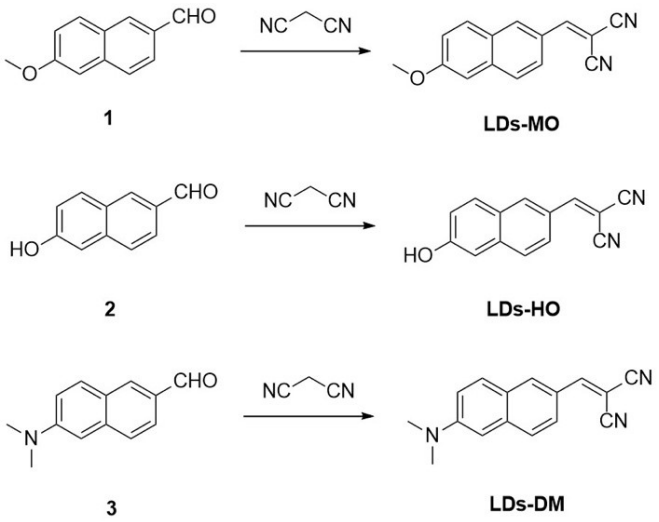

Scheme S1. Synthesis of LDs-MO, LDs-HO and LDs-DM

Synthesis of LDs-MO. A mix of 6-methoxy-2-naphthaldehyde (186 mg, 1 mmol), malononitrile (132 mg, 2 mmol) and 20 μL piperidine in 10 mL of absolute ethanol was refluxed for 3 h. After it was cooled to room temperature, the crystal was collected and washed by cold ethanol to afford **LDs-MO** (184.2 mg, 78.7 % yield). ^{1}H NMR (400 MHz, $CDCl_3$) δ (ppm): 8.19 (1H, d, J = 1.2 Hz), 8.06 (1H, dd, J_1 = 2.0 Hz, J_2 = 8.8 Hz), 7.82 (3H, dd, J_1 = 9.2 Hz, J_2 = 12.0 Hz), 7.24 (1H, m), 7.17 (1H, d, J = 2.4 Hz), 3.97 (3H, s). ^{13}C NMR (100 MHz, $CDCl_3$) δ (ppm): 161.59, 160.13, 138.43, 135.01, 131.88, 128.74, 128.46, 126.97, 125.53, 121.20, 114.86, 113.75, 106.60, 80.68, 56.10. HR-ESI-MS m/z: calcd 235.0866, found 235.0865 $[M + H]^+$.

Synthesis of LDs-HO. A mix of 6-hydroxy-2-naphthaldehyde (172 mg, 1 mmol), malononitrile (132 mg, 2 mmol) and 20 μL piperidine in 10 mL of absolute ethanol was refluxed for 3 h. After it was cooled to room temperature, the precipitate was collected and washed by cold ethanol to afford **LDs-HO** (181.3 mg, 82.4 % yield). ^{1}H NMR (400 MHz, DMSO-d_6)) δ (ppm): 10.57 (1H, s), 8.50 (1H, s), 8.32 (1H, d, J = 1.6 Hz), 7.99 (1H, dd, J_1 = 2.0 Hz, J_2 = 8.8 Hz), 7.92 (1H, m), 7.85 (1H, d, J = 8.8 Hz), 7.21 (2H, m). ^{13}C NMR (100 MHz, DMSO-d_6) δ (ppm): 161.11, 159.35, 137.67, 135.29, 131.960, 127.39, 126.59, 125.97, 124.05, 120.33, 114.88, 113.97, 109.37, 78.05. HR-ESI-MS m/z: calcd 219.0564, found 219.0560 $[M - H]^-$.

Synthesis of LDs-DM. A mix of 6-(dimethylamino)-2-naphthaldehyde (199 mg, 1 mmol), malononitrile (132 mg, 2 mmol) and 20 μL piperidine in 10 mL of absolute ethanol was refluxed for 3 h. After it was cooled to room temperature, the crystal was collected and washed by cold ethanol to afford **LDs-DM** (89.5 mg, 36.2 % yield). ^{1}H NMR (400 MHz, $CDCl_3$) δ (ppm): 8.06 (1H, s), 7.96 (1H, dd, J_1 = 1.6 Hz, J_2 = 8.8 Hz), 7.76 (1H, d, J = 9.2 Hz), 7.69 (1H, s), 7.62 (1H, d, J = 8.8 Hz), 7.16 (1H, dd, J_1 = 2.8 Hz, J_2 = 9.2 Hz), 6.85 (1H, d, J = 2.8 Hz), 3.17 (6H, s). ^{13}C NMR (100 MHz, $CDCl_3$) δ (ppm): 159.76, 151.68, 138.87, 135.86, 131.85, 127.62, 125.61, 125.48, 125.08, 116.95, 115.70, 114.54, 105.80, 40.84. HR-ESI-MS m/z: calcd 248.1182, found 248.1182 $[M + H]^+$.

3. Fig. S1 ^{1}HNMR, ^{13}CNMR of compounds

^{1}HNMR of LDs-MO

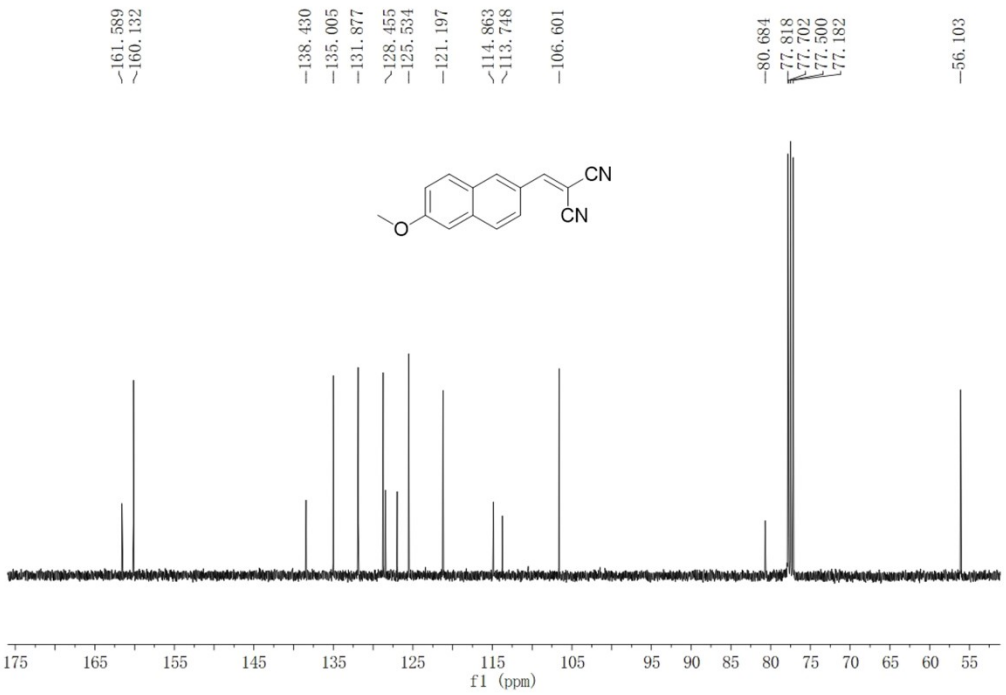

^{13}CNMR of LDs-MO

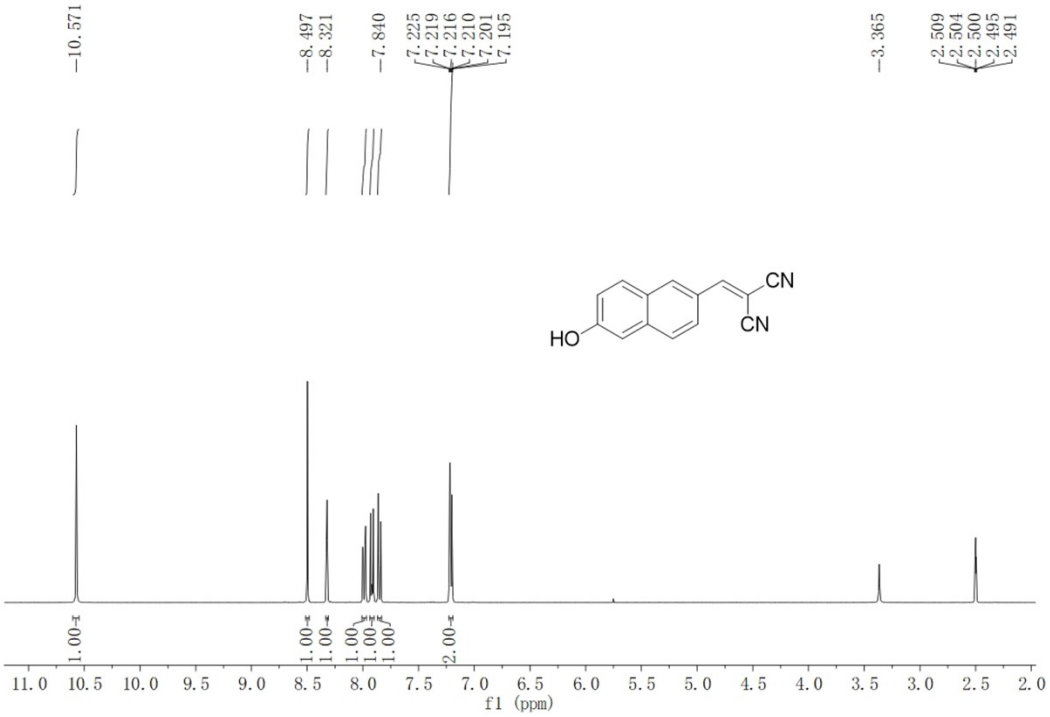

^{1}HNMR of LDs-HO

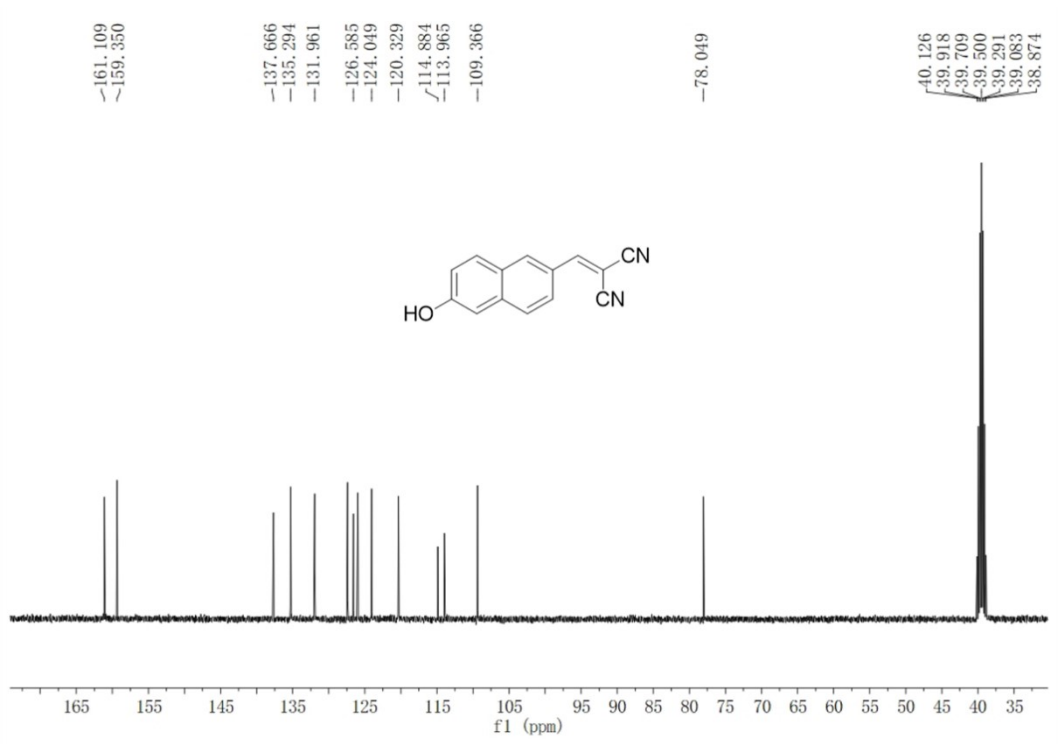

^{13}CNMR of LDs-HO

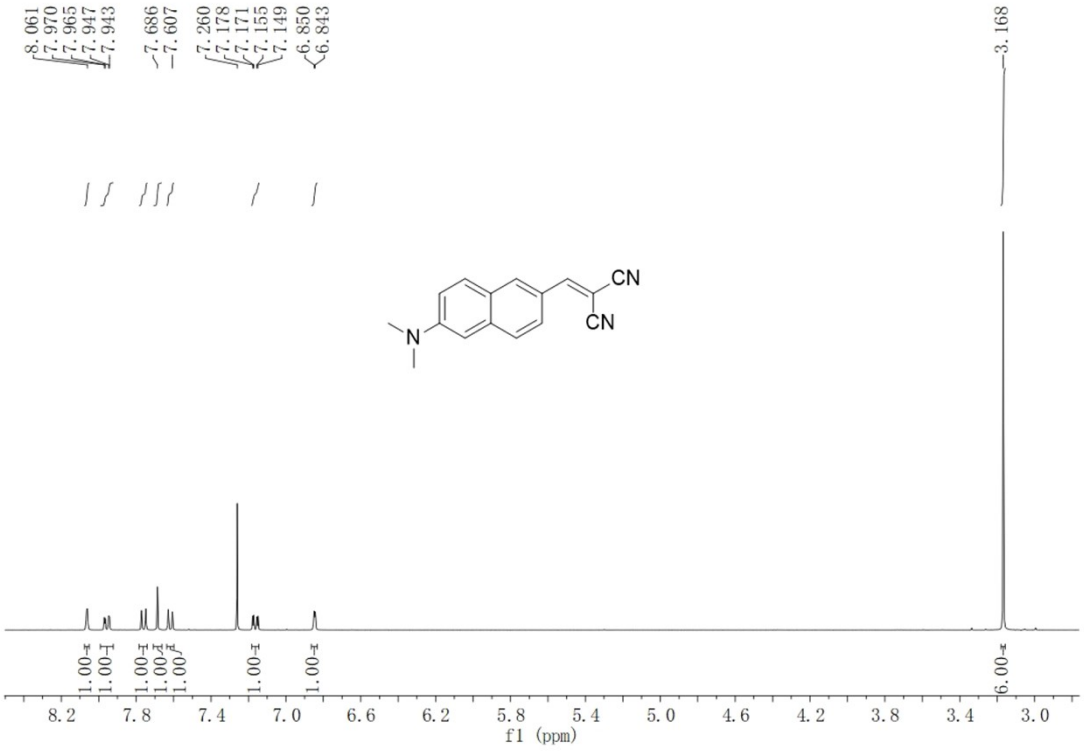

^{1}HNMR of LDs-DM

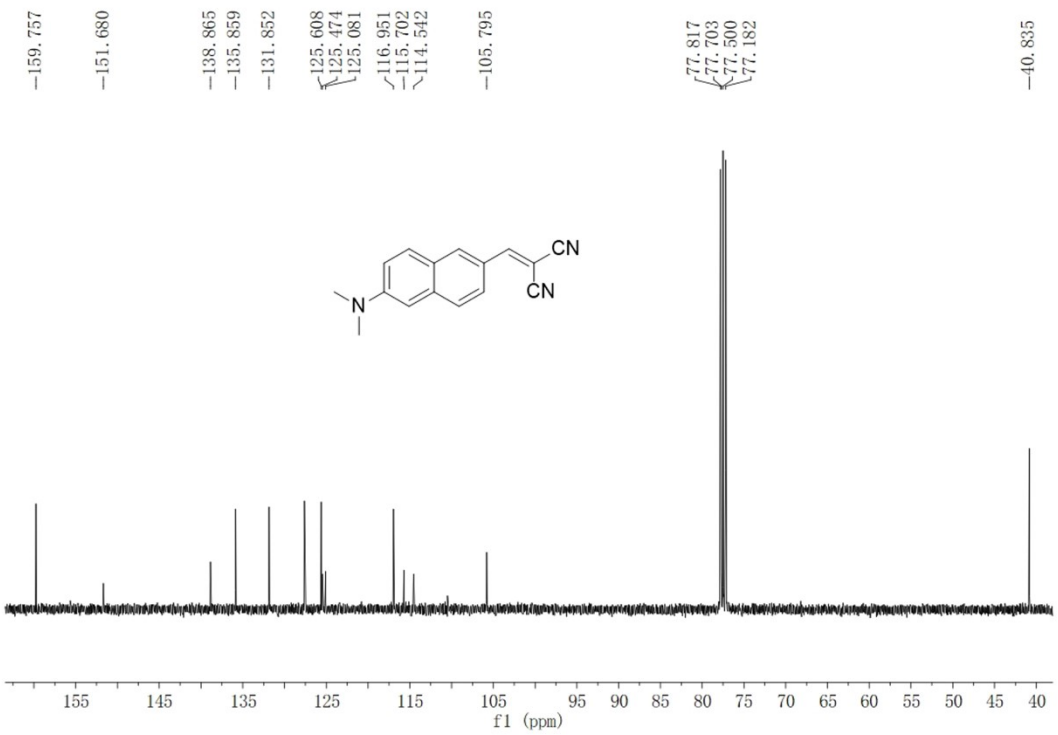

^{13}CNMR of LDs-DM

4. Table. S1. The photophysical properties of **LDs-DM**, **LDs-HO** and **LDs-MO** in the different solvents. $E_T(30)$ is the empirical parameter for solvent polarity.

LDs-DM

Solvents	$E_T(30)$	λ_{abs}/nm	λ_{em}/nm	Stokes shift/ nm
Toluene	33.9	458	523	65
Dioxane	36.0	450	543	93
EtOAc	38.1	454	559	105
Acetone	42.2	460	590	130
DMSO	45.1	476	611	135
H_2O	63.1	420	707	287

LDs-HO

Solvents	$E_T(30)$	λ_{abs}/nm	λ_{em}/nm	Stokes shift/ nm
Toluene	33.9	398	455	57
Dioxane	36.0	374	469	95
EtOAc	38.1	376	471	95
Acetone	42.2	386	480	94
DMSO	45.1	396	499	103
H_2O	63.1	354	531	177

LDs-MO

Solvents	$E_T(30)$	λ_{abs}/nm	λ_{em}/nm	Stokes shift/ nm
Toluene	33.9	384	435	51
Dioxane	36.0	374	450	76
EtOAc	38.1	374	452	78
Acetone	42.2	368	457	89
DMSO	45.1	378	486	108
H_2O	63.1	350	534	184

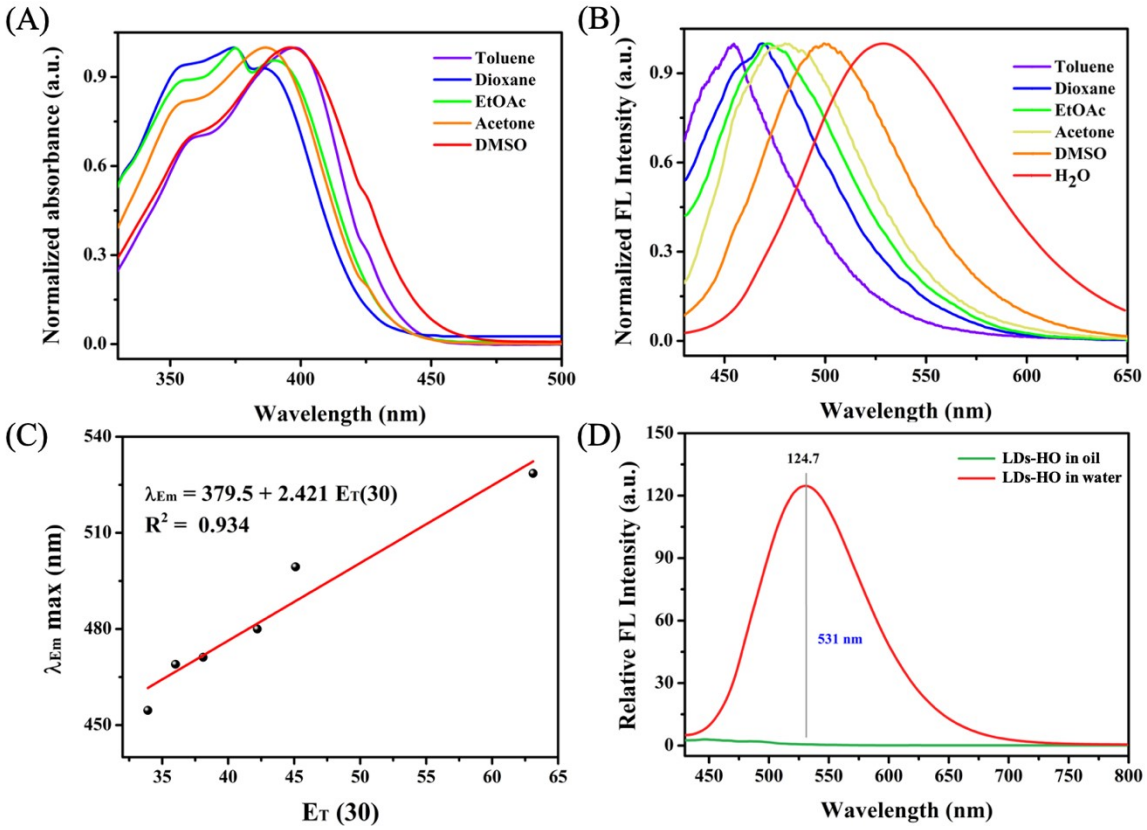

5. Fig. S2 The photophysical properties of **LDs-HO**. (A) The absorbance of **LDs-HO** in different solvents. (B) The fluorescence of **LDs-HO** in different solvents. (C) Linear relationship between the maximum emission wavelength of **LDs-HO** and the solvent's polarity. (D) The fluorescence of **LDs-HO** in oil and water. (λ_{ex} = 410 nm, 10 μM)

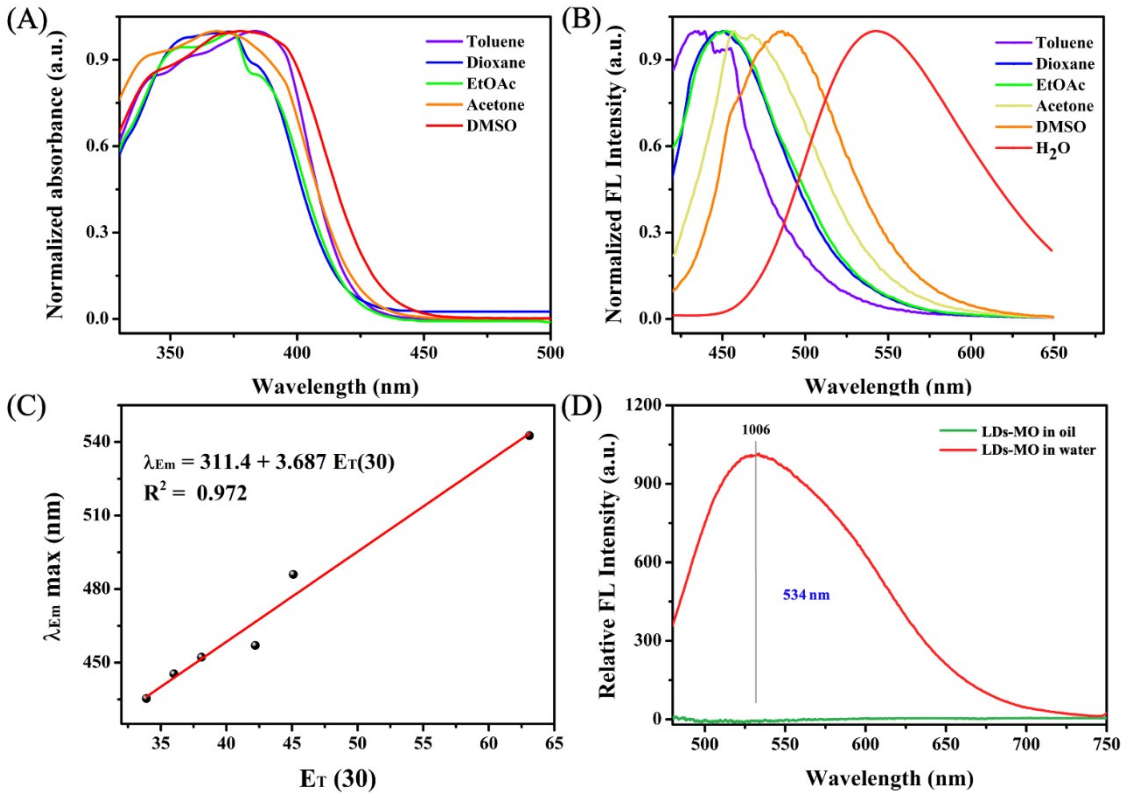

6. Fig. S3 The photophysical properties of **LDs-MO**. (A) The absorbance of **LDs-MO** in different solvents. (B) The fluorescence of **LDs-MO** in different solvents. (C) Linear relationship between the maximum emission wavelength of **LDs-MO** and the solvent's polarity. (D) The fluorescence of **LDs-MO** in oil and water. (λ_{ex} = 380 nm, 10 μM)

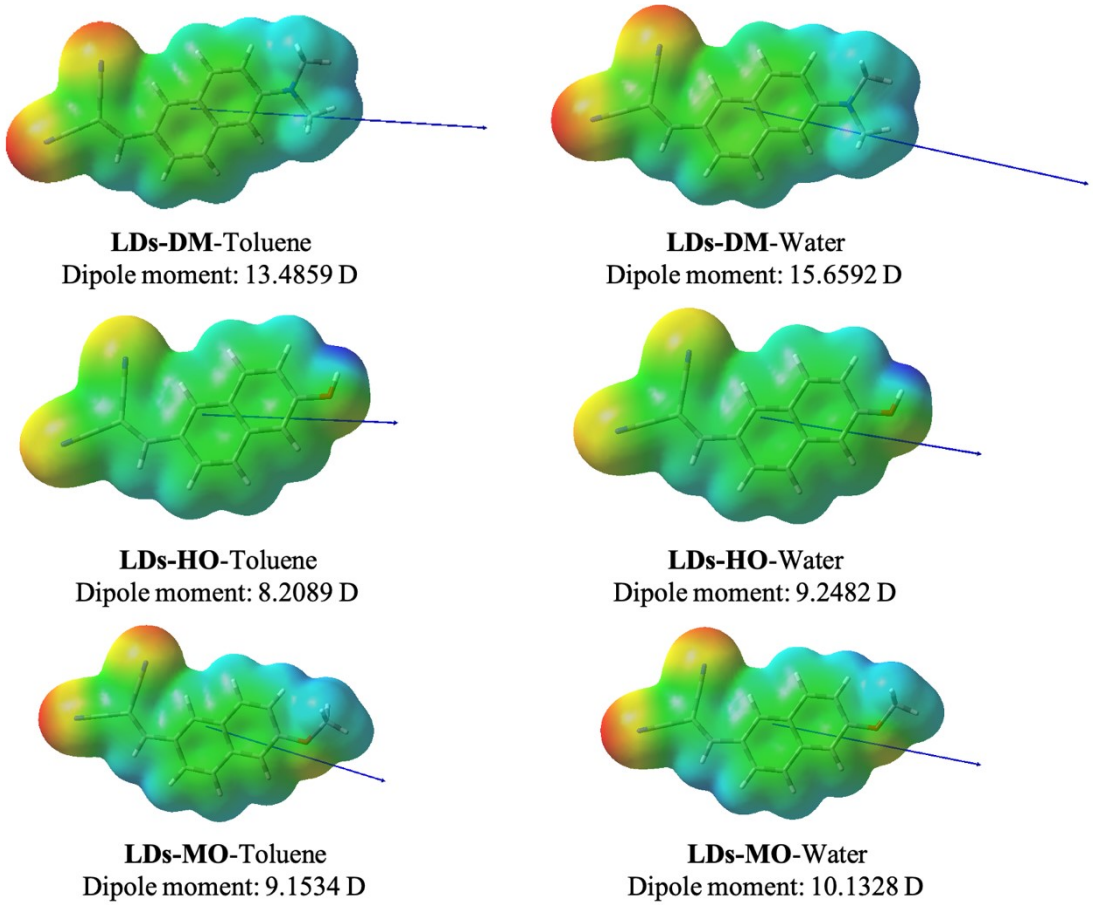

7. Fig. S4 The dipole moment of **LDs-DM**, **LDs-HO** and **LDs-MO** in toluene and water.

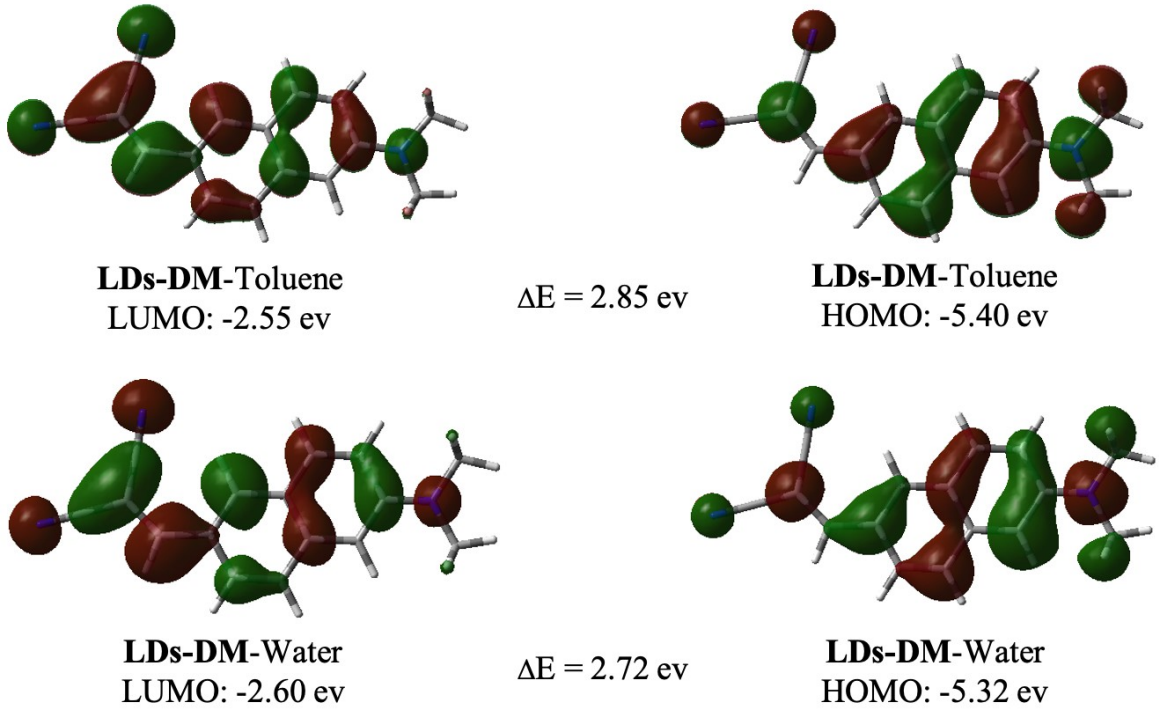

8. Fig. S5 The HOMO and LUMO energy level of **LDs-DM** in toluene and water.

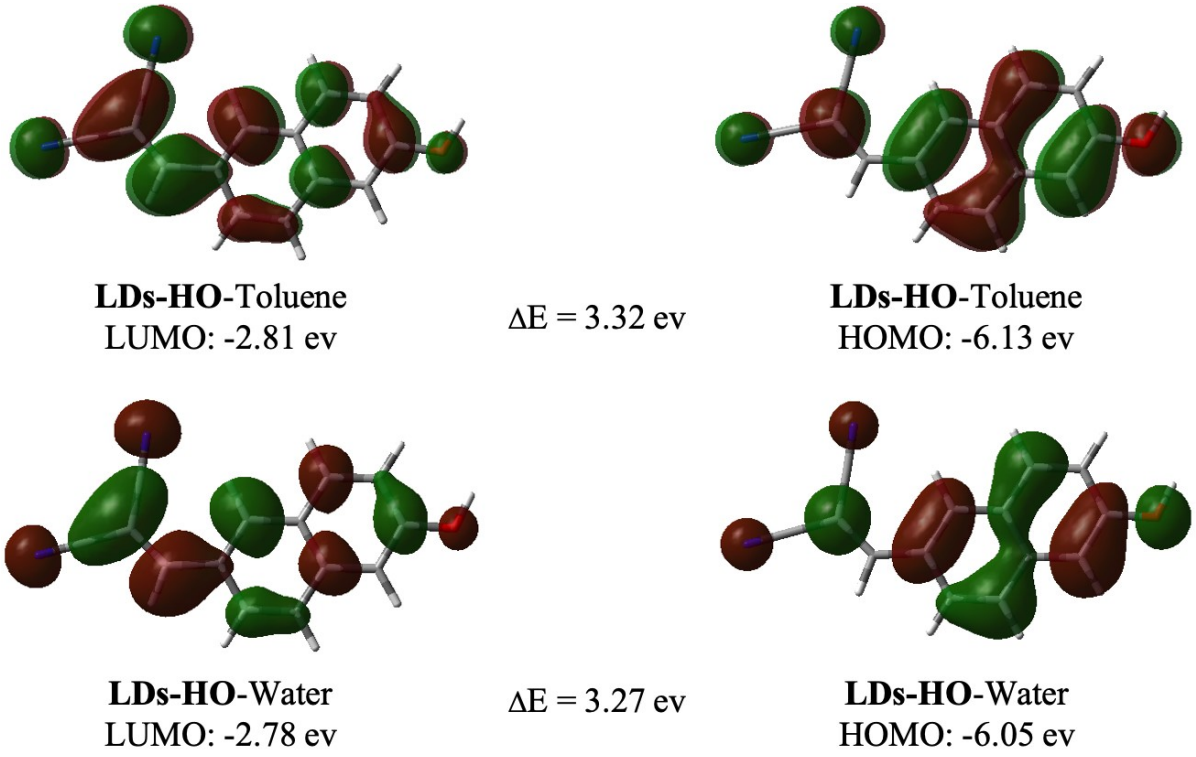

9. Fig. S6 The HOMO and LUMO energy level of **LDs-HO** in toluene and water.

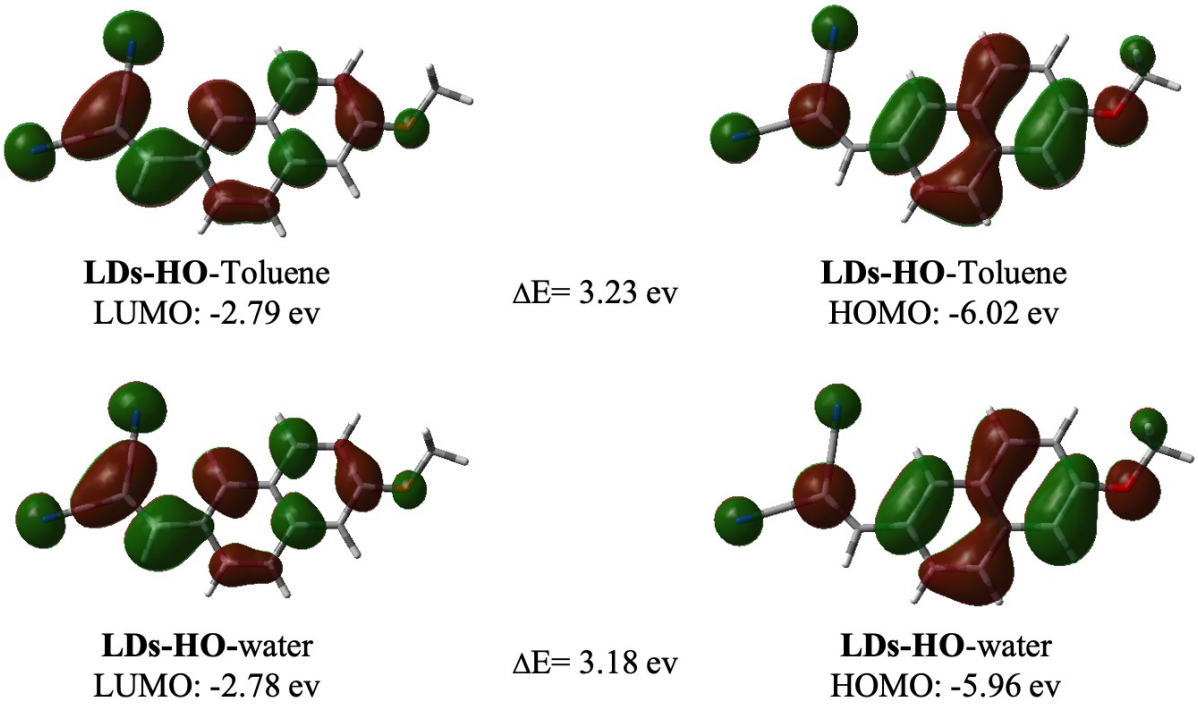

10. Fig. S7 The HOMO and LUMO energy level of **LDs-MO** in toluene and water.

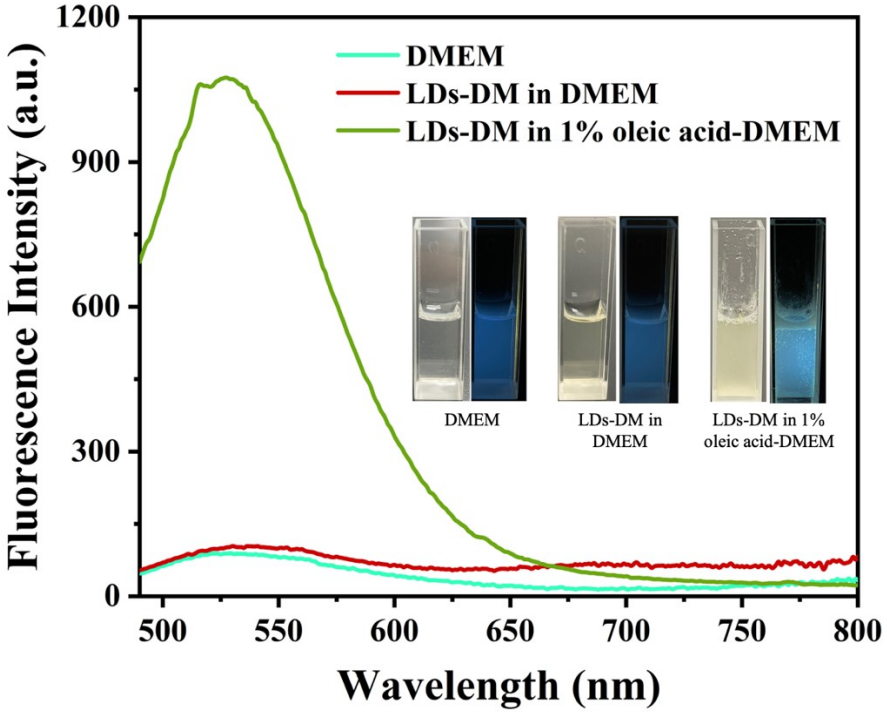

11. Fig. S8 The fluorescence spectra of **LDs-DM** (10 μM) in the presence and absence of oleic acid in FBS free DMEM without phenol red. Insert the image of white light and UV light.

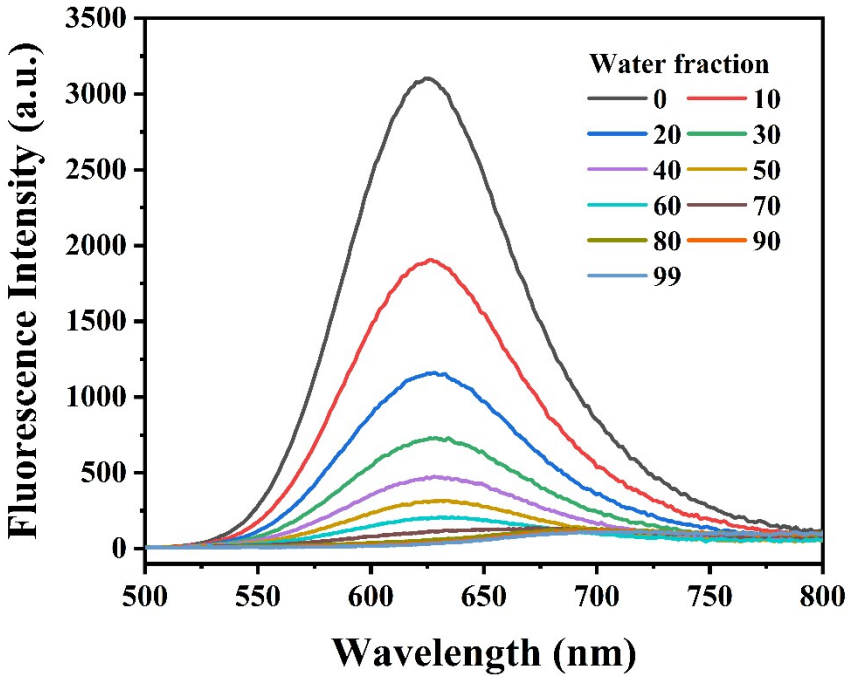

12. Fig. S9 The fluorescence spectra of **LDs-DM** (10 μM) in the different water fractions.

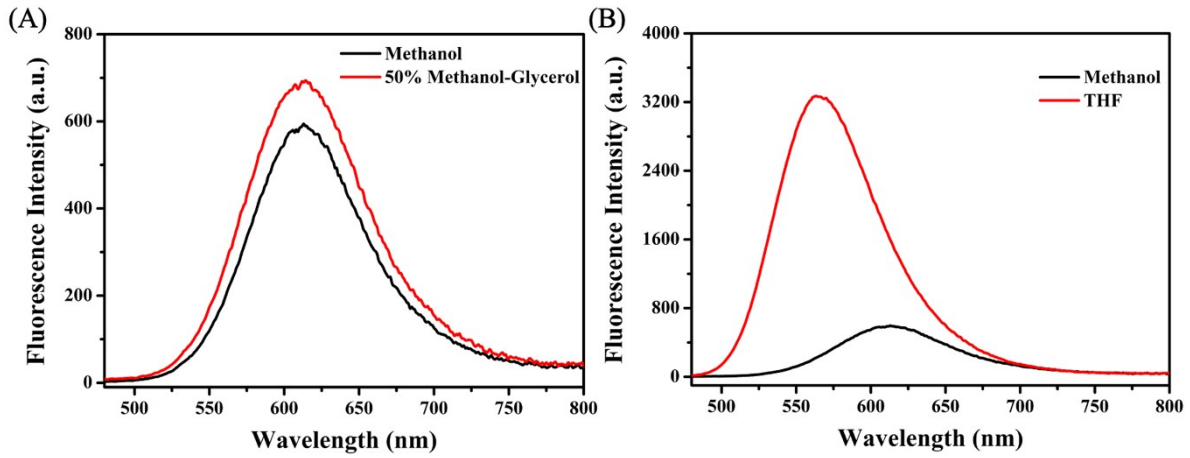

13. Fig. S10 (A) The fluorescence spectra of **LDs-DM** under different viscosity in methanol and glycerol system. (B) The fluorescence spectra of **LDs-DM** in THF and methanol. THF and methanol have almost the same viscosity (0.53 cP vs 0.60 cP) but different polarity ($E_T(30)$ = 37.4 vs 55.4)..

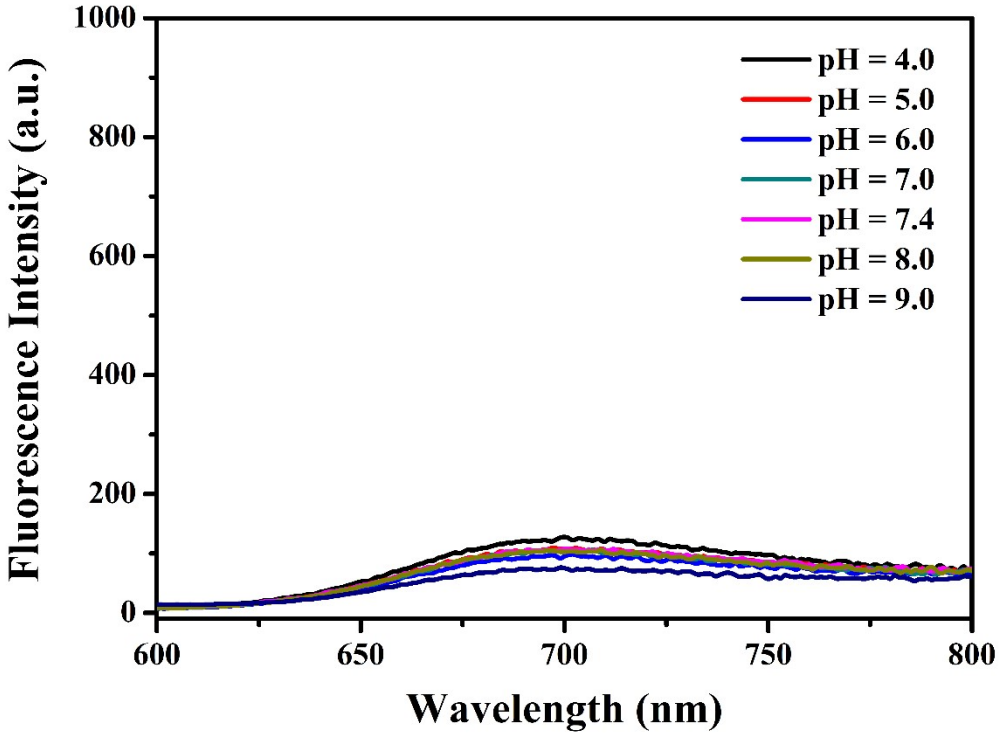

14. Fig. S11 The fluorescence spectra of **LDs-DM** in different PBS buffer solvents.

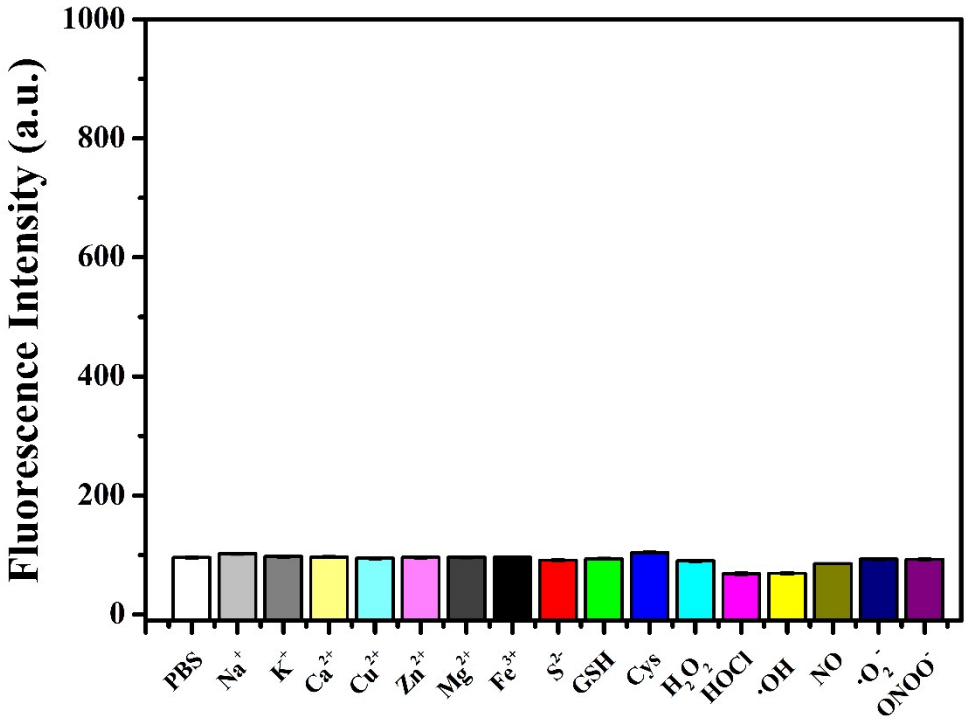

15. Fig. S12 The fluorescence intensity of **LDs-DM** (10 μM) to various relevant analytes in phosphate buffer (pH 7.4, 10 mM). 100 μM (Na^+, K^+, Ca^{2+}, Cu^{2+}, Zn^{2+}, Mg^{2+}, Fe^{3+}, S^{2-}, GSH, Cys); 50 μM (H_2O_2, HOCl, ·OH, NO, $·O_2^-$, $ONOO^-$).

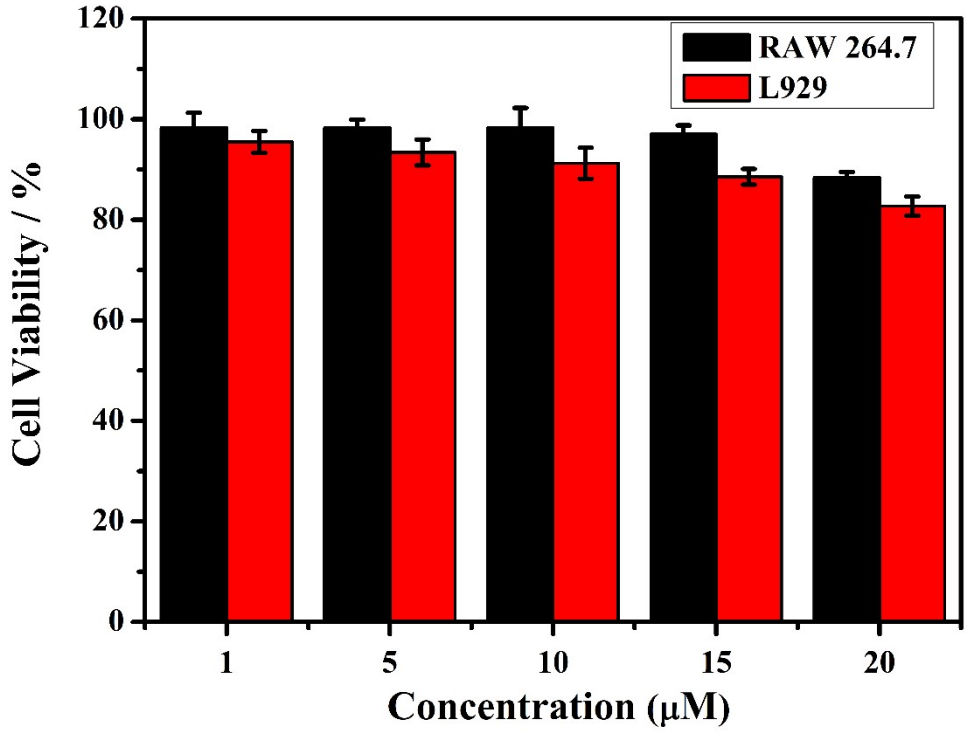

16. Fig. S13 Cell viability of L929 and RAW 264.7 treated with different concentrations of **LDs-DM**.

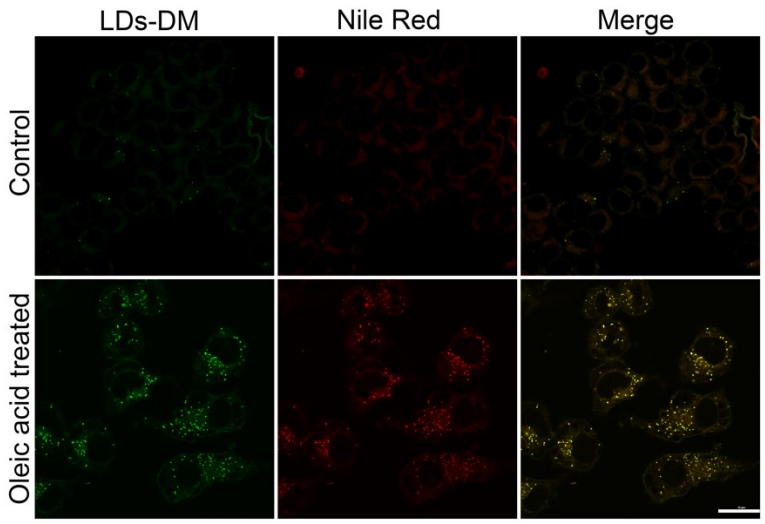

17. Figure S14 Imaging of RAW 264.7 cells with or without oleic acid pretreated stained with **LDs-DM** (1 μM, λ_{ex} = 488 nm, λ_{em} = 500-550 nm) and Nile red (1 μM, λ_{ex} = 488 nm, λ_{em} = 570-620 nm). Scale bar is 25 μm.

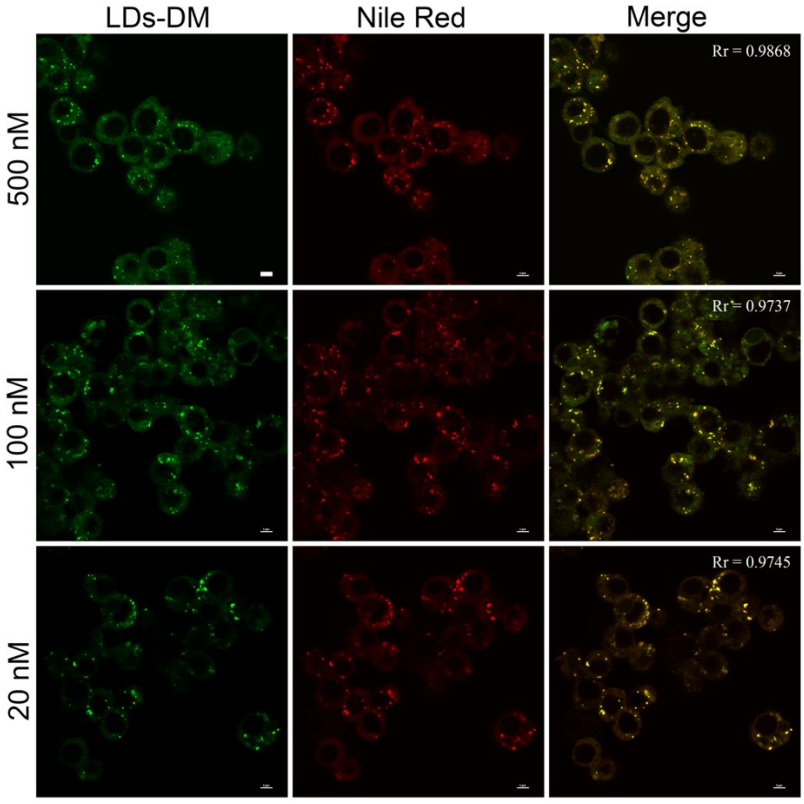

18. Fig. S15 Colocalization imaging of 10 μM oleic acid pretreated RAW 264.7 cells stained with different concentrations of **LDs-DM** (λ_{ex} = 488 nm, λ_{em} = 500-550 nm) and Nile red (1 μM, λ_{ex} = 488 nm, λ_{em} = 570-620 nm). Rr represented the Pearson's coefficient. Scale bar is 25 μm

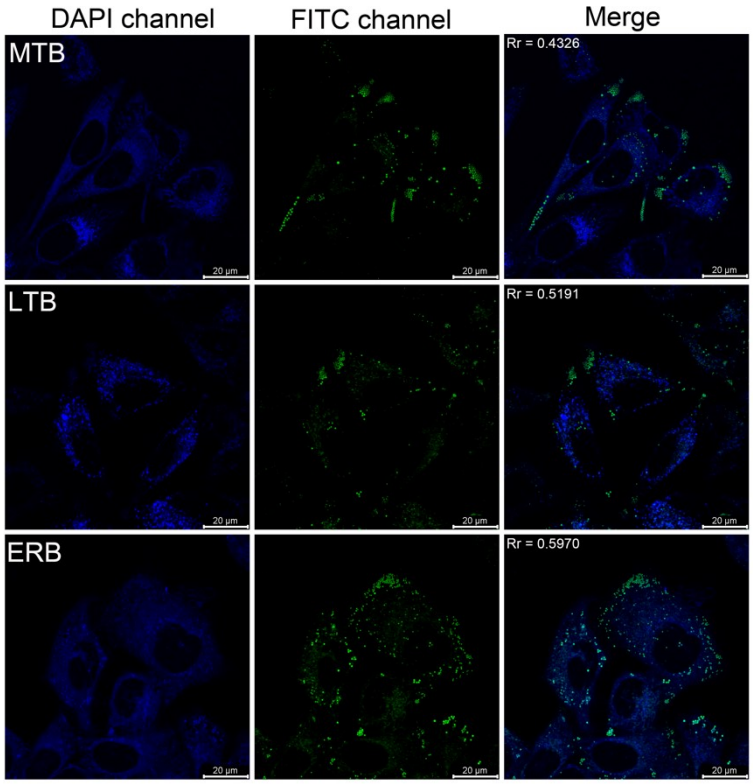

19. Fig. S16 Colocalization imaging of oleic acid pretreated (10 μM, 1 h) HeLa cells stained with of LDs-DM (500 nM, λ_{ex} = 488 nm, λ_{em} = 500-550 nm, FITC channel) and Mito-tracker Blue (MTB, 1 μM), Lyso-tracker Blue (LTB, 1 μM) and ER-tracer Blue (ERB, 1 μM), respectively. (λ_{ex} = 405 nm, λ_{em} = 430-470 nm, DAPI channel). Rr represented the Pearson's coefficient. Scale bar is 20 μm.

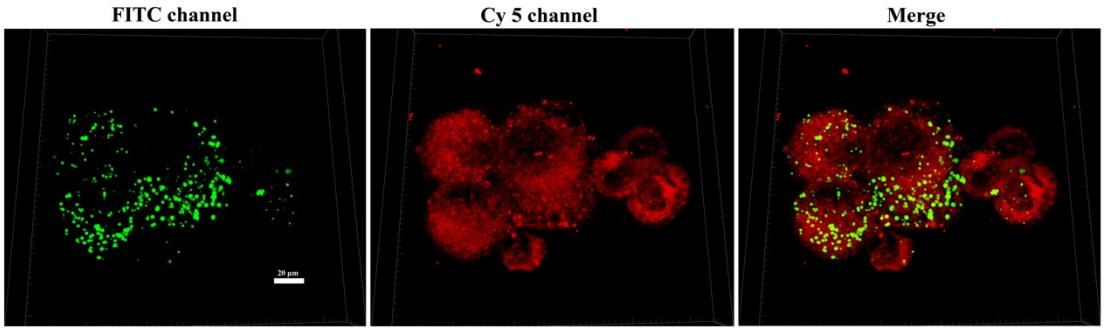

20. Fig. S17 Simultaneous dual-color 3D imaging of 10 μM oleic acid pretreated RAW 264.7 cells co-incubation with **LDs-DM** (500 nM). For FITC channel, λ_{ex} = 488 nm, λ_{em} = 500-550 nm; for Cy 5 channel, λ_{ex} = 488 nm, λ_{em} = 663-738 nm. Scale bar is 20 μm.

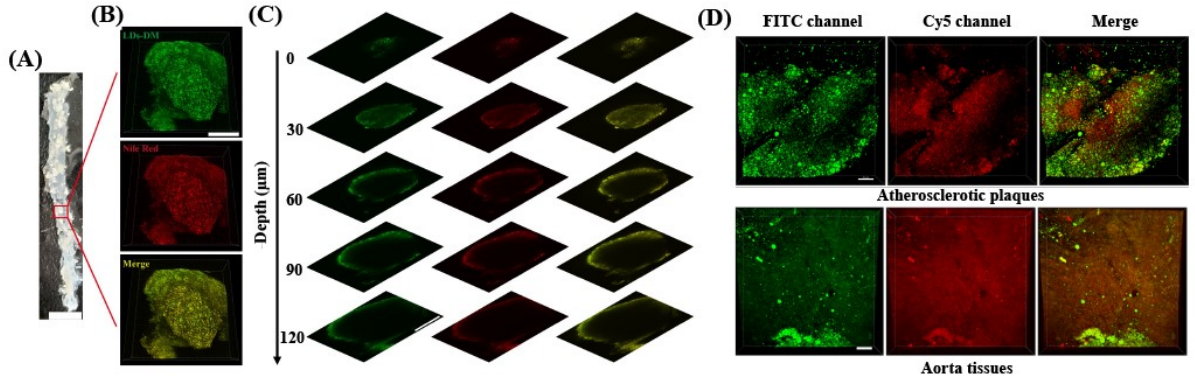

21. Fig. S18 (A) En face photograph of the opened aorta from an ApoE-/- mouse, scale bar is 5 mm. (B) Simultaneous 3D imaging of the microstructures of atherosclerotic plaques stained with **LDs-DM** (500 nM) and Nile red (1 μM), scale bar is 200 μm. (C) Images of the atherosclerotic plaques stained with **LDs-DM** (500 nM) and Nile red (1 μM) at different imaging depths, scale bar is 200 μm. (D) Simultaneous dual-color 3D imaging of the microstructures of atherosclerotic plaques and aorta tissue stained with 500 nM **LDs-DM** within lumen (500-550 nm for FITC channel) and (663-738 nm for Cy5 channel) under single excitation at 488 nm, scale bar is 70 μm.

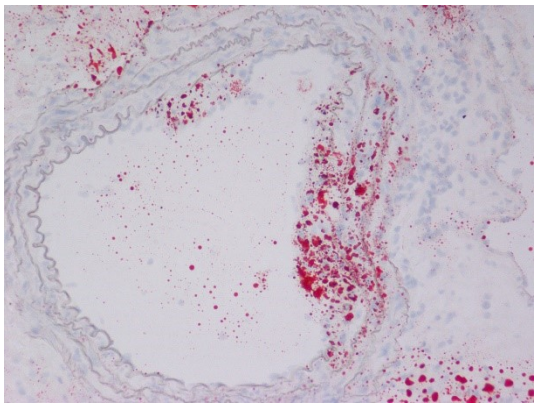

22. Fig. S19 Section of an ApoE$^{-/-}$ mouse's aortic vessel stained by Oil Red O (200×).

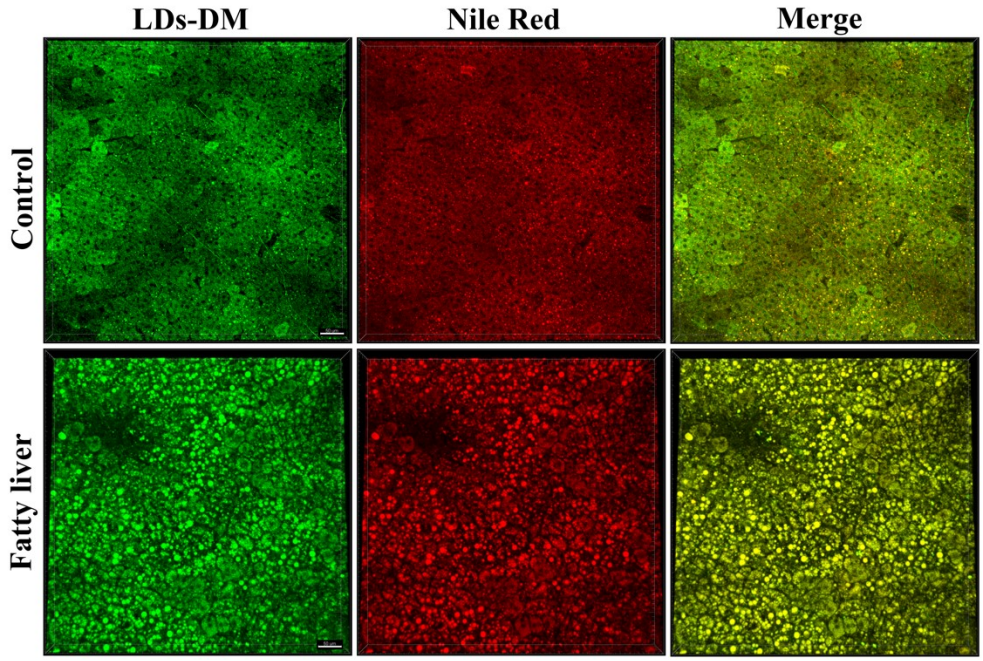

23. Fig. S20 3D imaging of hepatic tissues of fatty liver mice and normal mice stained with **LDs-DM** (500 nM, λ_{ex} = 488 nm, λ_{em} = 500-550 nm) and Nile red (1 μM, λ_{ex} = 488 nm, λ_{em} = 570-620 nm). Scale bar is 50 μm.